Received: 19 January 2025 | Revised: 7 March 2025 | Accepted: 21 March 2025 | Published online: 26 March 2025

RESEARCH ARTICLE

Smart Wearable Technology
2025, Vol. 00(00) 1–7
DOI: 10.47852/bonviewSWT52025252

BON VIEW PUBLISHING

An IoT-enabled Deep Learning Approach Implemented on Android Device for Automated Identification of Breast Cancer Using Thermal Images

Adnan Altaf[1] and Rajesh Kumar Tripathy[1,*]

[1]*Department of Electronics and Electrical Engineering, Birla Institute of Technology and Science (BITS), Pilani, Hyderabad Campus, India*

Abstract: Breast cancer (BC) is a very common type of cancer in women, and it occurs due to the abnormal growth of breast cells to produce malignant tumors. The early detection of BC is challenging in clinical standards to reduce the fatality rate caused by this disease. Artificial intelligence is helpful in early and automated detection of BC and provides a cost-effective way to assist radiologists in providing better diagnostic decisions. The artificial intelligence (AI) model integrated with the Internet of Things (IoT) provides the framework for real-time analysis of patient data and tele-healthcare monitoring for detecting BC. This paper proposes a novel IoT-enabled deep learning-based approach implemented on an Android device to detect BC using thermal images. A deep convolutional neural network (CNN) architecture with five blocks of cascaded convolutions followed by max-pooling after each block and cascaded dense layers is formulated and trained using the Google Cloud central processing unit. The post-training quantization (PTQ) of deep CNN (DPCNN) is performed using floating-point 16-bit (FP16) and integer 8-bit (INT 8)-based quantization techniques. The reduced-size DPCNN model is deployed on a cloud framework and an Android device for real-time detection of BC using thermal images. The DPCNN model deployed on the Android device provides a portable framework for low latency, enhanced privacy, and offline processing compared to the cloud-based framework for detecting BC using thermal images. The experimental results obtained using a public database reveal that the proposed DPCNN has obtained the accuracy values of 99.63% and 99.27% for FP16 and INT8 cases to detect BC. The proposed DPCNN model has fewer parameters and higher classification performance than transfer learning and existing methods in detecting BC using thermal images.

Keywords: breast cancer, thermal images, CNN, accuracy, android implementation, IoT

1. Introduction

Breast cancer (BC) is a lethal disease that arises from abnormal cell growth within the breast tissue, leading to the formation of malignant tumors [1]. According to the World Health Organization data, more than 2.3 million women globally are diagnosed with BC [2]. In India, the number of BC cases is significantly increasing each year [3]. Detecting BC in the early stage is essential for effective treatment and improved chances of recovery [4]. Different imaging methods, such as thermography, mammography, and ultrasonography, are used to diagnose BC [1, 5]. Thermography is particularly advantageous because it is a non-contact imaging test that can detect BC based on changes in temperature patterns. It is well-suited for dense breast tissue and does not expose patients to ionizing radiations like in mammography [6]. The advances of the Internet of Things (IoT) and deep learning (DL) [7] enable the development and implementation of smart healthcare systems for the automated identification of BC using thermal images. Such a system benefits remote monitoring and telemedicine applications. The on-device implementation of DL models helps reduce the dependency on cloud services and maintains the privacy and security of patient data and offline accessibility [7]. The Android application provides a user-friendly interface for real-time detection of BC using thermal images. Developing a novel and lightweight DL model and its real-time implementation on cloud framework and android-based edge devices is interesting for smart healthcare applications to detect BC using thermal images.

In the last decade, various techniques based on machine learning (ML) and DL have been utilized to automatically identify BC using thermal images [1]. Acharya et al. [8] have used the texture features of thermal images and the support vector machine (SVM) classifier to detect BC. Milosevic et al. [9] extracted the gray-level co-occurrence matrices-based features from the thermal images and used the K-nearest neighbor classifier to detect BC. Similarly, Francis et al. [10] have evaluated the statistical features in the curvelet transform domain of thermal images and used the SVM classifier for detecting BC. In another study, Pramanik et al. [11]

*Corresponding author: Rajesh Kumar Tripathy, Department of Electronics and Electrical Engineering, Birla Institute of Technology and Science (BITS), Pilani, Hyderabad Campus, India. Email: tripathyrk@hyderabad.bits-pilani.ac.in

computed the discrete wavelet transform domain features from thermal images and used a multi-layer feed-forward neural network to detect BC. Similarly, EtehadTavakol et al. [12] used the higher-order spectral invariant features of thermal images and the AdaBoost classifier to detect BC. The classification performance of the ML-based methods to detect BC is heavily dependent on the extraction of raw features such as statistical, texture, and shape from thermal images. The ML-based methods also require the feature selection stage to choose the relevant features of thermal images for detecting BC. Similarly, Gade et al. [1] have investigated different transfer learning (TL) models to identify BC using thermal images recorded from different subjects. They found that the ResNet101 network demonstrated higher classification accuracy than other TL models in identifying BC using thermal images. Zuluaga-Gomez et al. [13] have developed a CNN architecture with Bayesian optimization-based selection of hyperparameters to detect BC using thermal images. Similarly, in [1], authors have formulated the multiscale image decomposition domain DL approach to detect BC using thermal images. They have demonstrated higher classification performance than Bayesian optimization-based DPCNN and various TL models in detecting BC. Nissar et al. [14] have used sharpened cosine similarity, CNN, and squeeze and excitation blocks-based DL architecture to detect BC using thermal images. Similarly, Chi et al. [15] used a ResNet34-based pre-trained block to extract features from thermal images and an SVM classifier to detect BC. The TL, multiscale-based DL, and Bayesian optimization-based DPCNN models have higher parameters in the inference phase in detecting BC using thermal images [1, 13]. The existing ML and DL-based models have not been implemented or deployed on edge devices for real-time detection of BC. Therefore, it is challenging to develop novel DL-based methods for accurate and real-time detection of BC using thermal images.

In recent years, lightweight DL models and their implementation on edge computing devices such as Android, microcontrollers, and field programmable gate arrays have been explored for different biomedical applications [7]. These models require fewer floating-point operations, reduced memory footprints, low latency, reduced power consumption, privacy, and security for edge computing applications [7]. The quantization and pruning operations are helpful in further reducing the size of the DL models for implementing these models on edge devices [7, 16]. The lightweight DL models have not been explored for detecting BC on Android-based edge devices using thermal images. The novelty of this work is to develop a novel DPCNN model architecture with fewer parameters than the existing DL techniques for detecting BC with input as thermal images. The important contributions of this work are as follows:

1) A novel DPCNN architecture based on triple convolution max-pooling drop-out batch normalization (TCMPDBN) blocks is proposed for the detection of BC using thermal images.
2) The Performance of the DPCNN model is evaluated for subject-dependent and subject-independent validation strategies.
3) The Quantization of the weight parameters and activation functions of DPCNN is performed using FP16 and INT 8-based quantization techniques.
4) The reduced-size quantized DPCNN model is deployed on an Android device for real-time detection of BC using thermal images from different subjects.

The remaining sections of this paper are arranged as follows. In Section 2, we describe the details of the database containing thermal images. The proposed DL model architecture and the details regarding the implementation of this model on Android devices are written in Section 3. The results and discussion parts are written in Section 4. The conclusions of this letter are given in Section 5.

2. Thermal Image Database

This work has used the thermal images from a public database [17] to assess the performance of the proposed DPCNN model for detecting BC. This database includes 1520 thermal images from 56 subjects.

From each subject, 20 thermal images have been recorded sequentially within an interval of 15 s [17]. The thermal images are recorded using a FLIR thermal camera with temperature and sensitivity ranges of $[-40^{\circ}C, 500^{\circ}C]$, and $< 0.04^{\circ}C$, respectively [17]. In the database, the dimension of each thermal image is given as 640 × 480. The 760 thermal images (380 left breast and 380 right breast thermal images) from 19 subjects have been given for the healthy or normal class. Similarly, the 720 thermal images from 36 subjects are specified for the cancerous class. In the database, 40 thermal images are given for one subject of cancerous class. In this work, 1520 thermal images are used to develop and evaluate the suggested DPCNN model to identify BC.

3. Proposed Method

The structural representation of the proposed method to detect BC using thermal images is depicted in Figure 1. Initially, the image resizing is performed to reduce the size of the original thermal image into 64 × 64. Larger size-based thermal images can increase the number of parameters of the DPCNN model o detect BC. We have also considered the thermal images of sizes as 256 × 256 and 128 × 128 to estimate the classification results of the DPCNN model for detecting BC. The optimal size of the thermal image is determined using the accuracy of the DPCNN model.

3.1. Proposed DPCNN model

The architecture of the proposed DPCNN model for identifying BC using thermal images is depicted in Figure 2(a). The DPCNN model contains five TCMPDBN blocks and four dense or fully

Figure 1
Block diagram of the proposed approach for detecting BC using the thermal image

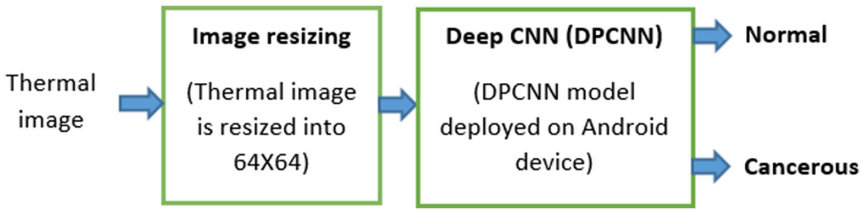

Figure 2
Architecture of the suggested DPCNN for detecting BC using thermal images

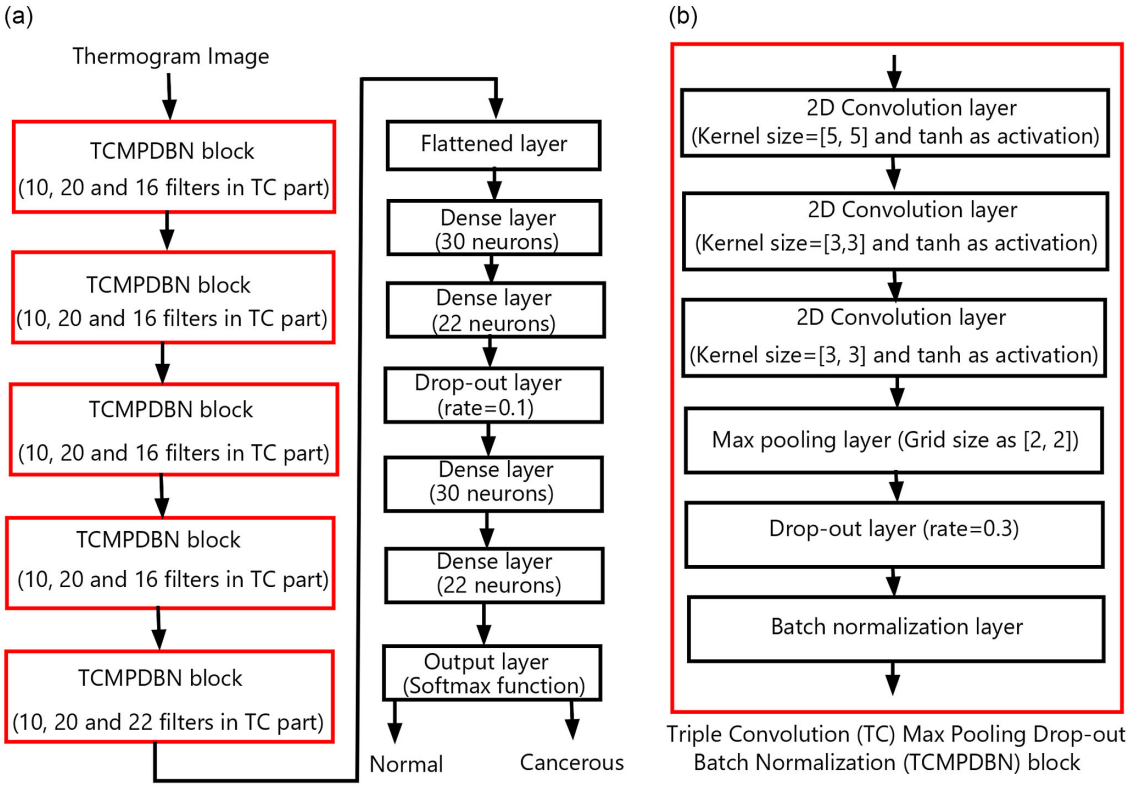

connected layers. A drop-out layer is added after the first two dense layers of the presented DPCNN model architecture. The output layer consists of two neurons (softmax activation) with the encoded vectors as [1, 0] for the normal class and [0, 1] for the cancerous class, respectively. The architecture of each TCMPDBN block is depicted in shown in Figure 2(b). Each TCMPDBN block comprises three convolution layers followed by max-pooling, drop-out, and batch normalization layers. In the convolution layers, the "tanh" activation function is used. Similarly, for dense layers, the rectified linear unit activation function has been employed. The k^{th} feature map produced after the l^{th} two-dimensional (2D) convolution layer is presented as follows [18]:

$$F_{c,d}^{k,l} = f\left(\sum_{i=0}^{I-1}\sum_{j=0}^{J-1}\sum_{m=1}^{M} K_{i,j,m}^{k} X_{c.s+i,\, d.s+j,m}^{(l-1)} + b^{k}\right) \quad (1)$$

where $X_{i,\,j,m}^{(l-1)}$ is the m^{th} feature map in the $l-1$ $^{\text{th}}$ layer. The $K_{i,j,m}^{k}$ and b^{k} are the kernel matrix and bias values for k^{th} feature map. s is the stride along the height and width direction of the image or feature map. Similarly, in the max-pooling layer, k^{th} feature map, $\widetilde{F}_{c,d}^{k,l}$ is evaluated as follows [18]:

$$\widetilde{F}_{c,d}^{k,l} = max_{i=0}^{k_h-1} max_{i=0}^{k_w-1}\left[F_{c.s+i,d.s+j}^{k,l}\right] \quad (2)$$

where s is the stride of the pooling operation. k_{h} and k_{w} are the height and width of the pooling window. $F_{c.s+i,d.s+j}^{k,l}$ is the input feature map given to the 2D max-pooling layer. In this work, the k_{h} and k_{w} are considered as 2. The drop-out and batch normalization are also used in the TCMPDBN block. The drop-out factor of 0.3 is considered. This means that 30% of neurons are randomly set as zero during the training of the proposed DPCNN for the detection of BC. In the batch normalization layer, the activation values are normalized based on the batch size to improve training stability [19]. The hold-out validation, leave-one-out subject-independent CV (LOOSICV), and 5-fold cross-validation (CV) strategies are utilized to choose the training and test instances (thermal images) of the proposed DPCNN model [1]. For the LOOSICV case, the thermal images of one subject are used to test the DPCNN model, whereas the remaining subject's thermal images are utilized in the training phase of the model. The same procedure is repeated for each subject in the LOOSICV case, and the accuracy measure of the DPCNN model is evaluated for each subject. The training hyperparameters of the proposed DPCNN model are cost function as categorical cross entropy, optimizer as "Adam" (initial learning rate equal to 0.0005), number of epochs as 400 (early stopping with patience as 50 epochs), and batch size as 64, respectively. These hyperparameters are obtained using the grid-search to maximize the accuracy of the validation thermal images for detecting BC [1, 19]. The classification measures such as precision, $F1$-score, recall, and accuracy are evaluated for the DPCNN model with 5-fold CV and hold-out validation strategies for detecting BC using thermal images. Furthermore, we have compared the classification results obtained using the suggested DPCNN with different TL models such as MobileNetV2 [20], EfficientNetV2B3 [21], VGG19 [22], and ResNet101 [23] for detecting BC using thermal images. The last layer of these pre-trained models is removed, and the new layer containing two neurons is connected at the output of each model [1]. In the fine-tuning phase, only the last layer weight and bias parameters of each TL model are updated using the backpropagation algorithm. For each TL model, the number of epochs and initial learning rate values as 100 (early stopping with

patience as 20 epochs) and 0.001 are used [1]. The proposed DPCNN and the existing TL models are implemented using the Python framework with the TensorFlow (Keras) package [24].with different TL models such as MobileNetV2 [20], EfficientNetV2B3 [21],

3.2. Deployment of DPCNN

The proposed DPCNN model has been deployed in an Android device to identify BC using thermal images. Similarly, we have also deployed the suggested DPCNN model on a web application (WAPP) for the IoT-enabled automated identification of BC using thermal images. The streamlit-cloud-based framework is utilized for deploying the Python code and the parameters of the proposed DPCNN model files to prepare the WAPP [7]. The Android studio-based framework is utilized to create the mobile application (MAAP) to test the DPCNN model detecting BC using thermal images. The TensorFlow Lite is integrated with Android Studio using Java or Kotlin, which enables the creation of MAAP for real-time detection of BC using thermal images.

The PTQ is applied to reduce the model size so that the DPCNN model can be deployed on the Android device. The FP16 and INT8-based quantization cases [25] are used to obtain reduced precision representations of weight parameters and activation functions of the DPCNN model. The accuracy values of the suggested DPCNN model are evaluated for FP16 and INT8-based quantization cases.

4. Results and Discussion

The results of the DPCNN model to detect BC using different validation cases (hold-out and 5-fold CV) are depicted in Table 1. It is observed that for both validation cases, the DPCNN model has produced classification accuracy values of more than 99% to detect BC using thermal images. Similar variations are also observed in other performance measures of the DPCNN model. The confusion matrix of the DPCNN for the hold-out validation case is displayed in Table 2. The true positives for normal and cancerous classes are 136 and 137, respectively. Only one false positive is obtained using the DPCNN model to identify BC using thermal images. The saliency maps of the presented DPCNN model evaluated using the thermal images for normal and cancerous classes are displayed in Figure 3(a) and (b), respectively. It is noted that the morphologies of saliency maps are dissimilar for cancerous and normal classes, respectively. Hence, the proposed DPCNN model learns to produce different feature maps for cancerous and normal classes using input as thermal images. We have also calculated the classification accuracy of the suggested DPCNN model by considering the thermal images with sizes 128 × 128 and 256 × 256 for detecting BC. The accuracy values of DPCNN for thermal images of sizes 128 × 128 and 256 × 256 are obtained as 98.54% and 98.17%, respectively. The DPCNN model has produced higher classification accuracy using thermal images with sizes 64 × 64. The accuracy value of each subject evaluated using the DPCNN model with LOO subject-independent CV is depicted in Figure 4. It is noted that the DPCNN model has delivered the accuracy values of 100% for 42 subjects. The mean accuracy value of the DPCNN model for LOO subject-independent CV is 92.85%.

Table 2
Confusion matrix evaluated using DPCNN to detect BC

		Actual		
		Normal	Cancerous	Total
Predicted	Normal	136	0	136
	Cancerous	1	137	138
	Total	137	137	

Figure 3
(a) Saliency map computed using DPCNN model for normal class and (b) saliency map computed using DPCNN model for the cancerous class

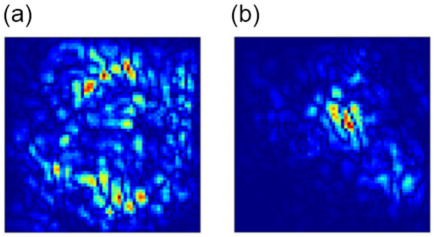

Figure 4
Variations of accuracy values of DPCNN with number of subjects for detection of BC using LOO subject-independent cross-validation strategy

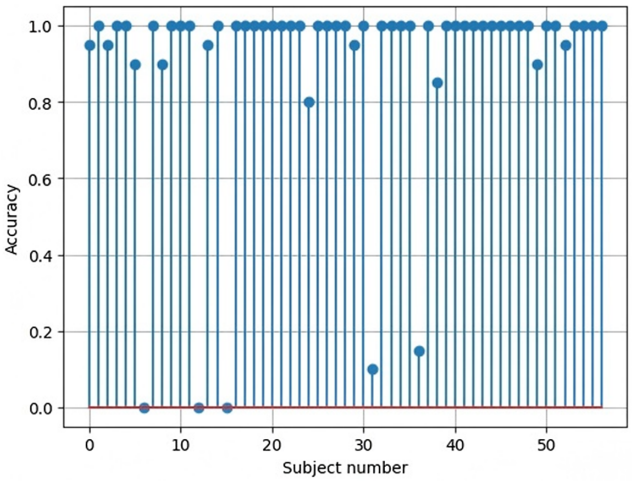

Table 1
Performance of DPCNN to identify BC for different validation cases

Validation	Accuracy (%)	Precision (%)	Recall (%)	*F*1-score (%)
Hold-out	99.45 ± 0.18	99.27 ± 0.73	99.64 ± 0.36	99.45 ± 0.19
5-fold CV	99.53 ± 0.26	99.47 ± 0.49	99.60 ± 0.52	99.53 ± 0.26

Table 3
Performance of DPCNN model with different quantization cases for weight parameters

Quantization case	Accuracy(%)	Model size
FP32	99.63	159.68KB
FP16	99.63	95.24KB
INT8	99.27	62.56KB

Figure 5
(a) Deployment of DPCNN model on an Android device for the detection of normal class using thermal image and (b) deployment of DPCNN model on an Android device to detect cancerous class using thermal image

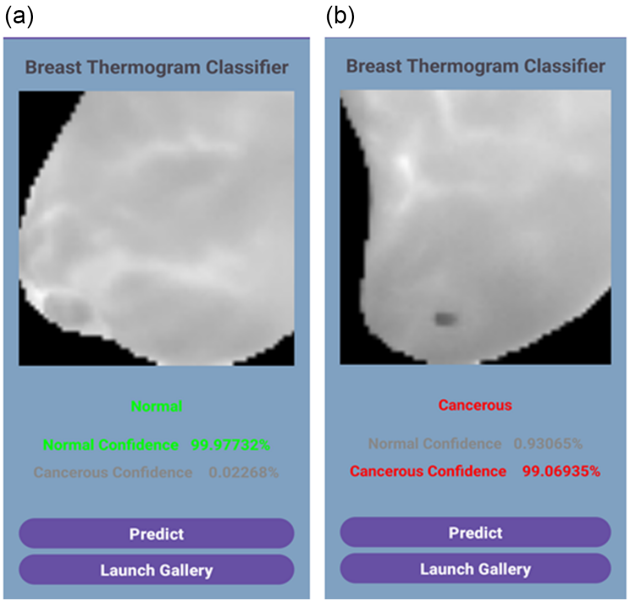

We have computed the accuracy of the DPCNN model using INT8 and FP16-based PTQ cases, and these results are displayed in Table 3 for hold-out validation. It is noted that the DPCNN with INT8-based quantization case has delivered an accuracy value of 99.27%. The DPCNN model size has been reduced from 159.68KB to 62.56KB when the INT8 quantization case is used. The INT8-based quantized version of the DPCNN model has been deployed on an Android device and a WAPP for real-time detection of BC. The inferences of the Android-based implementation of DPCNN models for normal and cancerous classes are depicted in Figure 5(a) and (b), respectively. Similarly, we have shown the inferences of the WAPP-based DPCNN models for normal and cancerous classes in Figure 6(a) and (b), respectively. The DPCNN model has successfully detected the normal and cancerous classes on Android-based edge devices and IoT-enabled WAPP using breast thermal images.

The accuracy of the proposed DPCNN model has been compared with existing TL and DL-based techniques in Table 4 to detect BC using thermal images. It is observed that the VGG19 [22], MobileNetV2 [20], ResNet101 [23], and EfficientNetV2B3 [21]-based TL models have obtained accuracy values of less than 80% to detect BC. The total parameters of each TL model in the inference phase are more than 3 Million. The multiscale image decomposition domain DL method has an accuracy value of 99.54% to detect BC using thermal images [1]. However, this model has more than three times the total parameters of the proposed DPCNN model for detecting BC. Thus, the presented approach has obtained higher classification accuracy and has fewer parameters than all the TL and multiscale DL-based models to detect BC. The advantages of WAPP-based inference of the proposed DPCNN are cross-platform-based accessibility, real-time disease diagnosis, and telemonitoring [15]. Internet connectivity is required for the WAPP-based real-time inference of the DPCNN model to detect BC. The WAPP will not run without an internet connection in the computer or Android device. The MAPP-based inference of the proposed DPCNN model provides the edge device-based platform for the automated identification of BC using thermal images. Similarly, the advantages of MAPP-based inference of the DPCNN

Figure 6
(a) Deployment of DPCNN model on a web application to detect normal class using thermal image and (b) deployment of DPCNN model on a web application to detect cancerous class using thermal image

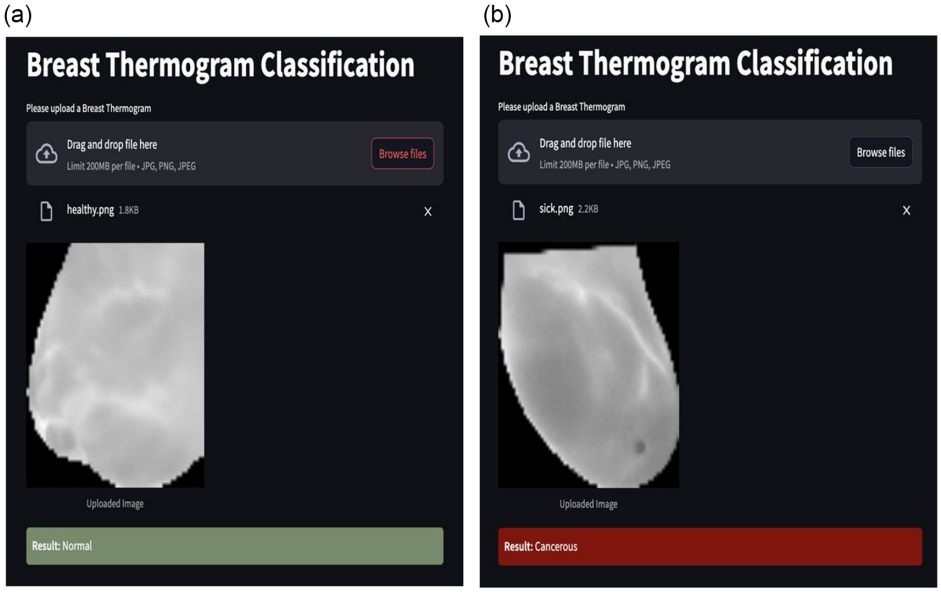

Table 4
Comparison with existing methods to detect BC using thermal images

Method utilized	Accuracy (%)	Total parameters
MobileNetV2-based model [20]	76.65	3, 538, 984
EfficientNetV2B3-based model [21]	73.63	13, 081, 152
VGG19-based model [22]	75.54	20, 074, 562
ResNet101-based model [23]	78.16	42, 858, 882
Multiscale image decomposition domain deep learning [1]	99.54	12, 2, 038
Proposed DPCNN model	99.63	35, 840

model are offline access, portability, and privacy of patient data (thermal images) [15]. Developing an integrated framework (integrating thermal camera with edge device) for real-time monitoring and inference of the DPCNN model to detect BC is very challenging. Regular weight updates in different layers of DPCNN using new patients' thermal image data help obtain optimal model parameters for detecting BC [26]. Weight updates or re-training using new patients' thermal image data can be performed in the cloud. The proposed IoT-enabled Android-based DPCNN system does not require the MAPP update, as the updated DPCNN model can be transferred from the cloud to the Android device. Federated learning (FDL) has the advantage of creating privacy-preserving AI models using sensor data from multiple locations [27]. The performance of the proposed DPCNN model can be evaluated using the thermal images recorded from patients from different locations or hospitals in an FDL environment for automated detection of BC.

5. Conclusion

A novel DPCNN model architecture using TCMPDBN blocks has been introduced in this paper to identify BC using thermal images automatically. This model has demonstrated an accuracy value of more than 99% in recognizing BC using thermal images. The accuracy value of the model has been reduced to 99.27% when the INT8-based PTQ has been performed. The DPCNN model has been deployed on the cloud-based framework for IoT-enabled real-time detection of BC using thermal images. The INT8-based reduced precision-based representation of the suggested DPCNN model is deployed on an Android device and WAPP for real-time identification of BC using thermal images. The DPCNN model has obtained higher accuracy for detecting BC using thermal images. The suggested DL model has fewer parameters in the inference phase than different TL architectures to identify BC. Future work can include testing the DPCNN model with diverse datasets containing thermal images for detecting BC.

Ethical Statement

This study does not contain any studies with human or animal subjects performed by any of the authors.

Conflicts of Interest

The authors declare that they have no conflicts of interest to this work.

Data Availability Statement

Data sharing is not applicable to this article as no new data were created or analyzed in this study.

Author Contribution Statement

Adnan Altaf: Conceptualization, Methodology, Software, Validation, Formal analysis, Data curation, Writing – original draft. **Rajesh Kumar Tripathy:** Investigation, Resources, Writing – review & editing, Visualization, Supervision, Project administration.

References

[1] Gade, A., Dash, D. K., Kumari, T. M., Ghosh, S. K., Tripathy, R. K., & Pachori, R. B. (2023). Multiscale analysis domain interpretable deep neural network for detection of breast cancer using thermogram images. *IEEE Transactions on Instrumentation and Measurement*, *72*, 1–13. https://doi.org/10.1109/TIM.2023.3317913

[2] World Health Organization. (2024). *Breast cancer* [Fact sheet]. Retrieved from: https://www.who.int/news-room/fact-sheets/detail/breast-cancer

[3] Kulothungan, V., Ramamoorthy, T., Sathishkumar, K., Mohan, R., Tomy, N., Miller, G. J., & Mathur, P. (2024). Burden of female breast cancer in India: Estimates of YLDs, YLLs, and DALYs at national and subnational levels based on the national cancer registry programme. *Breast Cancer Research and Treatment*, *205*(2), 323–332. https://doi.org/10.1007/s10549-024-07264-3

[4] Dey, A., & Rajan, S. (2023). Hue-preserved quantile-based global contrast enhancement of breast thermograms for abnormality detection. *IEEE Sensors Letters*, *7*(9), 1–4. https://doi.org/10.1109/LSENS.2023.3308087

[5] An, J., Abdus-Shakur, T., & Denis, M. (2023). Quantitative assessment of tissue stiffness using transfer learning ultrasound elastography: A breast cancer phantom study. *IEEE Sensors Letters*, *7*(10), 1–4. https://doi.org/10.1109/LSENS.2023.3307102

[6] Singh, D., & Singh, A. K. (2020). Role of image thermography in early breast cancer detection-past, present and future. *Computer Methods and Programs in Biomedicine*, *183*, 105074. https://doi.org/10.1016/j.cmpb.2019.105074

[7] Vinod, A., Guddati, P., Panda, A. K., & Tripathy, R. K. (2024). A lightweight deep convolutional neural network implemented on FPGA and android devices for detection of breast cancer using ultrasound images. *IEEE Access*, *2*, 179190–179203. https://doi.org/10.1109/ACCESS.2024.3506334

[8] Acharya, U. R., Ng, E. Y. K., Tan, J. H., & Sree, S. V. (2012). Thermography based breast cancer detection using texture features and support vector machine. *Journal of Medical Systems*, *36*(3), 1503–1510. https://doi.org/10.1007/s10916-010-9611-z

[9] Milosevic, M., Jankovic, D., & Peulic, A. (2014). Thermography based breast cancer detection using texture features and minimum variance quantization. *EXCLI Journal*, *13*, 1204–1215.

[10] Francis, S. V., Sasikala, M., & Saranya, S. (2014). Detection of breast abnormality from thermograms using curvelet transform based feature extraction. *Journal of Medical Systems*, *38*(4), 23. https://doi.org/10.1007/s10916-014-0023-3

[11] Pramanik, S., Bhattacharjee, D., & Nasipuri, M. (2015). Wavelet based thermogram analysis for breast cancer detection. In *2015 International Symposium on Advanced Computing and Communication*, 205–212. https://doi.org/10.1109/ISACC.2015.7377343

[12] EtehadTavakol, M., Chandran, V., Ng, E. Y. K., & Kafieh, R. (2013). Breast cancer detection from thermal images using bispectral invariant features. *International Journal of Thermal Sciences*, *69*, 21–36. https://doi.org/10.1016/j.ijthermalsci.2013.03.001

[13] Zuluaga-Gomez, J., Al Masry, Z., Benaggoune, K., Meraghni, S., & Zerhouni, N. (2020). A CNN-based methodology for breast cancer diagnosis using thermal images. *Computer Methods in Biomechanics and Biomedical Engineering: Imaging & Visualization*, *9*(2), 131–145. https://doi.org/10.1080/21681163.2020.1824685

[14] Nissar, I., Alam, S., & Masood, S. (2024). Computationally efficient LC-SCS deep learning model for breast cancer classification using thermal imaging. *Neural Computing and Applications*, *36*(26), 16233–16250. https://doi.org/10.1007/s00521-024-09968-5

[15] Nguyen Chi, T., Le Thi Thu, H., Doan Quang, T., & Taniar, D. (2024). A lightweight method for breast cancer detection using thermography images with optimized CNN feature and efficient classification. *Journal of Imaging Informatics in Medicine*. https://doi.org/10.1007/s10278-024-01269-6

[16] Guddati, P., Dash, S., & Tripathy, R. K. (2024). FPGA implementation of the proposed DCNN model for detection of tuberculosis and pneumonia using CXR images. *IEEE Embedded Systems Letters*, *16*(4), 445–448. https://doi.org/10.1109/LES.2024.3370833

[17] Silva, L. F., Saade, D. C. M., Sequeiros, G. O., Silva, A. C., Paiva, A. C., Bravo, R. S., & Conci, A. (2014). A new database for breast research with infrared image. *Journal of Medical Imaging and Health Informatics*, *4*(1), 92–100. https://doi.org/10.1166/jmihi.2014.1226

[18] Gonzalez, R. C. (2018). Deep convolutional neural networks [lecture notes]. *IEEE Signal Processing Magazine*, *35*(6), 79–87. https://doi.org/10.1109/MSP.2018.2842646

[19] Bishop, C. M., & Bishop, H. (2024). *Deep learning: Foundations and concepts* (1st ed). Switzerland: Springer. https://doi.org/10.1007/978-3-031-45468-4

[20] Sandler, M., Howard, A., Zhu, M., Zhmoginov, A., & Chen, L. C. (2018). MobileNetV2: Inverted residuals and linear bottlenecks. In *2018 IEEE/CVF Conference on Computer Vision and Pattern Recognition*, 4510–4520. https://doi.org/10.1109/CVPR.2018.00474

[21] Tan, M., & Le, Q. V. (2021). EfficientNetV2: Smaller models and faster training. In *Proceedings of the 38th International Conference on Machine Learning*, *139*, 10096–10106.

[22] Simonyan, K., & Zisserman, A. (2015). Very deep convolutional networks for large-scale image recognition. In *3rd International Conference on Learning Representations*, 1–14.

[23] He, K., Zhang, X., Ren, S., & Sun, J. (2016). Deep residual learning for image recognition. In *2016 IEEE Conference on Computer Vision and Pattern Recognition*, 770–778. https://doi.org/10.1109/CVPR.2016.90

[24] Shanmugamani, R. (2018). *Deep learning for computer vision: Expert techniques to train advanced neural networks using TensorFlow and Keras*. UK: Packt Publishing.

[25] Durmaz Incel, O., & Bursa, S. Ö. (2023). On-device deep learning for mobile and wearable sensing applications: A review. *IEEE Sensors Journal*, *23*(6), 5501–5512. https://doi.org/10.1109/JSEN.2023.3240854

[26] Amin, M., Shehwar, D., Ullah, A., Guarda, T., Tanveer, T. A., & Anwar, S. (2022). A deep learning system for health care IoT and smartphone malware detection. *Neural Computing and Applications*, *34*(14), 11283–11294. https://doi.org/10.1007/s00521-020-05429-x

[27] Su, L., & Lau, V. K. N. (2021). Hierarchical federated learning for hybrid data partitioning across multitype sensors. *IEEE Internet of Things Journal*, *8*(13), 10922–10939. https://doi.org/10.1109/JIOT.2021.3051382

How to Cite: Altaf, A., & Tripathy, R. K. (2025). An IoT-enabled Deep Learning Approach Implemented on Android Device for Automated Identification of Breast Cancer Using Thermal Images. *Smart Wearable Technology*. https://doi.org/10.47852/bonviewSWT52025252